Polarimetric Tornado Detection

ALEXANDER V. RYZHKOV, TERRY J. SCHUUR, AND DONALD W. BURGESS

Cooperative Institute for Mesoscale Meteorological Studies, The University of Oklahoma, Norman, Oklahoma

DUSAN S. ZRNIC

National Severe Storms Laboratory, Norman, Oklahoma

(Manuscript received 23 June 2004, in final form 23 November 2004)

ABSTRACT

Polarimetric radars are shown to be capable of tornado detection through the recognition of tornadic debris signatures that are characterized by the anomalously low cross-correlation coefficient ρ_{hv} and differential reflectivity Z_{DR}. This capability is demonstrated for three significant tornadic storms that struck the Oklahoma City, Oklahoma, metropolitan area. The first tornadic debris signature, based on the measurements with the National Severe Storms Laboratory's Cimarron polarimetric radar, was reported for a storm on 3 May 1999. Similar signatures were identified for two significant tornadic events during the Joint Polarization Experiment (JPOLE) in May 2003. The data from these storms were collected with a polarimetric prototype of the Next-Generation Weather Radar (NEXRAD). In addition to a small-scale debris signature, larger-scale polarimetric signatures that might be relevant to tornadogenesis were persistently observed in tornadic supercells. The latter signatures are likely associated with lofted light debris (leaves, grass, dust, etc.) in the inflow region and intense size sorting of hydrometeors in the presence of strong wind shear and circulation.

1. Introduction

Dual-polarization radar has been recognized as being an efficient tool for the classification of different hydrometeor types and discrimination between meteorological and nonmeteorological scatterers (Zrnic and Ryzhkov 1999; Vivekanandan et al. 1999). It is natural to assume that tornadic debris is composed of more or less randomly oriented particles with very irregular shapes and a refractive index that is different from that of hydrometeors, thereby producing much different signatures than hydrometeors. Randomly oriented scatterers are characterized by differential reflectivity Z_{DR} that is equal to zero. If large debris scatterers are not chaotically oriented and possess some degree of common orientation, then their Z_{DR} might be either positive or negative, depending on their size and the mean canting angle.

The linear depolarization ratio (LDR) and cross-correlation coefficient ρ_{hv} of tornadic debris should also be quite different from signatures that are associated with hydrometeors. Similar to other nonmeteorological scatterers, such as natural ground cover (trees, grass, etc.), biological scatterers (insects, birds, and bats), and military chaff, tornadic debris is expected to have a significantly higher LDR and lower ρ_{hv} than that which is typical for liquid or frozen hydrometeors. This is because debris particles have large sizes, very irregular nonspherical shapes, a high refractive index, and a low degree of common alignment.

A polarimetric tornadic debris signature was first reported by Ryzhkov et al. (2002a), based on the measurements with the National Severe Storms Laboratory (NSSL) Cimarron polarimetric radar in one of the storms that constituted the famous central Oklahoma tornado outbreak on 3 May 1999. After tornado touchdown, the signature at the tip of the hook echo for that storm was identified by a Z_{DR} that was close to zero and anomalously low values of ρ_{hv} (less than 0.5).

The capability of a dual-polarization radar to detect tornadoes was further tested during the Joint Polarization Experiment (JPOLE), which was designed to evaluate the engineering concept and data quality of the polarimetric KOUN Weather Surveillance Radar-1988 Doppler (WSR-88D) and to demonstrate the utility of polarimetric radar data and products to operational users. Two significant tornadic events were observed with the KOUN radar in the Oklahoma City metropolitan area in May 2003. Analysis of these two events provides evidence of the polarimetric signatures

Corresponding author address: Alexander V. Ryzhkov, CIMMS/NSSL, 1313 Halley Circle, Norman, OK 73069.
E-mail: alexander.ryzhkov@noaa.gov

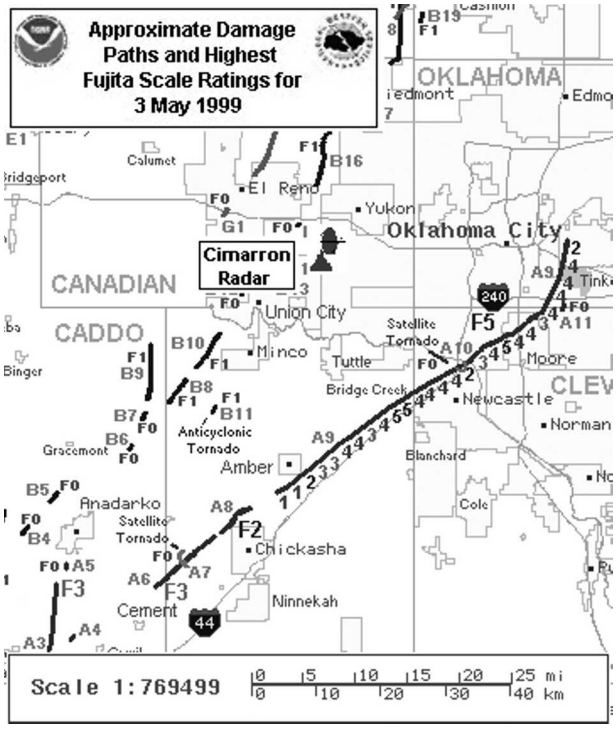

FIG. 1. Approximate damage paths and highest Fujita-scale ratings for the 3 May 1999 tornado outbreak.

that are associated with tornadic debris. The signatures looked very similar to the previous one observed with the Cimarron radar in 1999.

In this paper, we present polarimetric analyses of the three tornadic supercell storms that occurred in central Oklahoma on 3 May 1999, 8 May 2003, and 9 May 2003. Special attention is given to the polarimetric detection of tornadic touchdown that is associated with lofted debris. We also speculate about the possible interpretation of unusual polarimetric signatures that are observed elsewhere in tornadic storms, which might provide insight into microphysical aspects of tornadogenesis.

2. Tornadic case on 3 May 1999

Multiple tornadoes occurred in close proximity to the Oklahoma City metropolitan area on 3 May 1999 (Burgess et al. 2002). Approximate damage paths and highest Fujita-scale ratings for multiple storms within the Cimarron radar coverage area southwest of Oklahoma City are shown in Fig. 1. Polarimetric data from the Cimarron radar are available for the period from 2145 to 2322 UTC, after which time the radar went down after being hit by storm B (Fig. 1). Thus, the radar missed the most violent stage of storm A, which eventually struck the Oklahoma City metropolitan area. However, we have 15 volume scans of polarimetric data that include the developing stages of storms A and B, and a less destructive tornado rated as F3 in the Fujita scale (west of Chickasha, Oklahoma, in Fig. 1). This tornado produced an approximately 900-m-wide damage swath and lasted from 2246 to 2310 UTC. The tornado track was at the range of 45–60 km from the radar.

The 10-cm Cimarron radar measured the radar reflectivity factor Z at horizontal polarization, mean Doppler velocity V, Doppler spectrum width σ_v, differential reflectivity Z_{DR}, differential phase Φ_{DP}, and cross-correlation coefficient ρ_{hv} between radar returns at two orthogonal polarizations (Zahrai and Zrnic 1993). These data were collected at elevations of 0.0°, 0.5°, 1.5°, 2.5°, 4.0°, and 6.0°, with an update time of approximately 6 min. All radar variables were measured with a radial resolution of 0.24 km and an azimuthal resolution of about 1.9° (although the radar beam has 0.9° width). The 1.9° beam spacing resulted from a longer dwell time that was used to reduce statistical errors of polarimetric measurements.

It is important that we utilize the radar data collected at 0.0° elevation for which the center of the radar beam is as close to the ground as possible. At such a low elevation, the radar beam is inevitably partially blocked and the power-related radar variables such as Z and Z_{DR} are biased. Partial blockage, however, does not affect the phase-related variables: Doppler velocity and differential phase. Moreover, it is possible to restore correct values of Z and Z_{DR} by using the specific differential phase K_{DP} and the concept of self-consistency among Z, Z_{DR}, and K_{DP} in rain (Gorgucci et al. 1999). The self-consistency technique proves to work well even in the presence of severe beam blockage (Ryzhkov et al. 2002b). The Z and Z_{DR} data collected at 0.0° and 0.5° elevations have been corrected according to such a methodology.

After analysis of all 15 volume scans of data, we have selected the one that started at about 2305 UTC to illustrate tornadic polarimetric signatures. At that time, the F3 tornado was relatively close to the radar (within 55 km). Therefore, small-scale features can be more easily resolved. A combined plot of Z, V, Z_{DR}, and ρ_{hv} at the lowest plan position indicator (PPI) scan (0.0°) is shown in Fig. 2. The data in Fig. 2 have a resolution of 0.5 km $\times$ 0.5 km. A simple linear interpolation is used to convert the data from polar to Cartesian format in our study. Note that at longer distances from the radar a "physical" spatial resolution determined by the size of the radar sampling volume can be worse than 0.5 km.

At 2305 UTC, a hook echo was well developed and the area of hail mixed with rain is recognized north of the hook at $Y > -45$ km. The latter is marked with Z exceeding 60 dBZ near ground and 65 dBZ aloft. Maximal radar reflectivity within the hook is slightly below 50 dBZ. Intense cyclonic rotation at the tip of the hook is evident in the Doppler velocity image. Relatively poor azimuthal resolution of the radar data in this particular dataset (about 2°) does not allow us to distinguish the fine structure of velocity field in Fig. 2c. Nev-

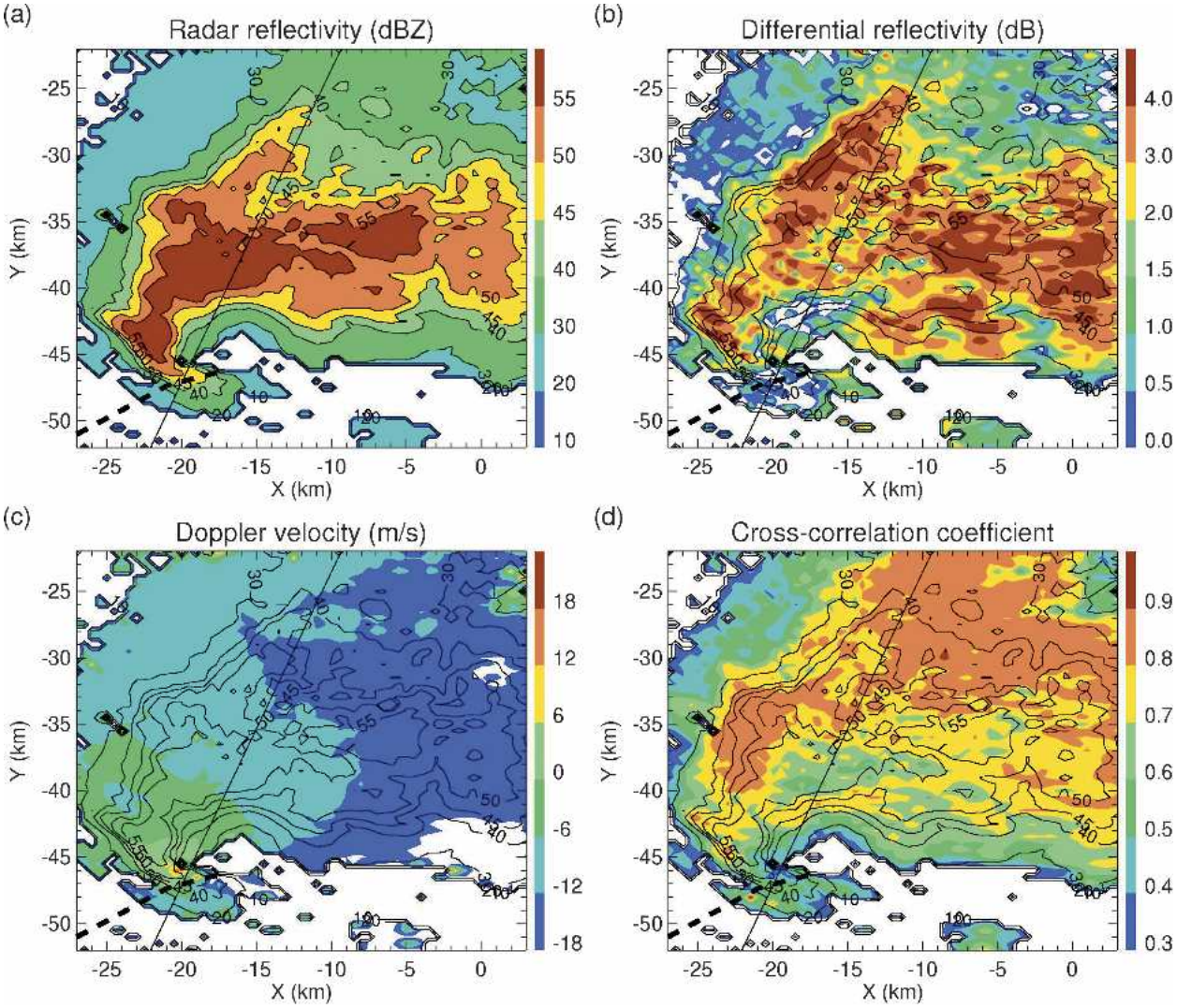

FIG. 2. Fields of Z, Z_{DR}, V, and ρ_{hv} at the lowest PPI scan (0.0°) at 2304 UTC 3 May 1999. Solid lines indicate azimuthal direction 203°, and dashed lines depict tornado track from the ground observations.

ertheless, analysis of individual adjacent radials shows that the azimuthal change in Doppler velocity is about 39 m s^{-1} across a distance of 2–3 km in the hook area.

As expected, differential reflectivity and the cross-correlation coefficient are anomalously low in the part of the hook where the tornado was detected (according to a ground survey, the tornado track is depicted by a thick dashed line in Fig. 2). Values of Z_{DR} (in decibels) are slightly positive or even negative at the tip of the hook. Such low Z_{DR} values can be explained by the presence of lofted debris in the radar resolution volume, and, to some extent, by enhanced differential attenuation along the propagation path that intersects the hail-bearing region northeast of the hook. Normally, Z_{DR} is corrected for differential attenuation using the empirical relation ΔZ_{DR} (dB) = $0.004\Phi_{DP}$ (°), which is valid at the S band for rain in Oklahoma (Ryzhkov and Zrnic 1995). Note the high Z_{DR} (more than 4 dB) in the area ahead of the forward-flank downdraft (FFD). Analysis of the vertical structure of Z_{DR} shows that the region of high Z_{DR} stretches above the freezing level in the updraft region (the "Z_{DR} column") and is very shallow (confined to a 1-km-depth layer) in the FFD area. The enhanced Z_{DR} in the updraft has been referred to as a Z_{DR} column (Conway and Zrnic 1993; Hubbert et al. 1998; Loney et al. 2002).

The cross-correlation coefficient drops below 0.4 at the inner side of the hook in the vicinity of the tornado track. Its minimal value is 0.25 at $X = -20.0$ km and $Y = -44.5$ km. The corresponding values of Z and Z_{DR} in that pixel are 43.2 dBZ and 0.0 dB, respectively. In pure rain or dry snow, ρ_{hv} usually varies between 0.980 and 0.997 if a dual-polarization radar is well designed. Because of quantization noise in the Cimarron data pro-

cessor, the measured values of ρ_{hv} are negatively biased, and those high values have never been attained. This should be taken into account in interpretation of the Cimarron polarimetric data. Although absolute values of ρ_{hv} are not reliable, its relative changes are more trustworthy. Notable are lower ρ_{hv} values (less than 0.7) within the 55-dBZ contour of Z (indicative of a rain–hail mixture) and at weaker reflectivities in the southern part of the storm that is associated with the updraft. The latter signature is very repetitive in the supercell storms and might indicate a mixture of raindrops and light debris (leaves, grass, etc.) being advected into the cloud by strong inflow.

Vertical cross sections of the three radar variables along the 203° azimuth (marked by a straight solid line in Fig. 2) are also revealing (see Fig. 3). A radar reflectivity maximum centered at a 1.5-km height (42-km range) is accompanied by low Z_{DR} and high ρ_{hv}. This combination of radar variables might indicate pure hail. In the area underneath, Z_{DR} sharply increases but ρ_{hv} decreases, which likely point to a mixture of hail and big raindrops with ice cores inside.

Within the hook, a tiny, shallow signature centered at 49.5 km from the radar and extending to less than 1 km above ground is visible. This signature is characterized by Z_{DR} close to 0 dB and ρ_{hv} less than 0.4. Very close proximity to the tornado track on the ground suggests that this signature is very likely associated with tornadic debris. Indeed, this is exactly what is expected for randomly oriented nonmeteorological scatterers with an irregular shape and high refractive index.

3. Tornadic case on 8 May 2003

During JPOLE, polarimetric data were collected with the KOUN WSR-88D—a prototype of a future polarimetric WSR-88D. The KOUN radar experiences much less blockage at lower elevations than the Cimarron radar and surpasses the latter in the quality of the polarimetric data. Values of ρ_{hv} measured by KOUN reach theoretical limits for rain (0.997–0.998) and confirm the high quality of the radar engineering design and radar data processor. Higher values of ρ_{hv} ensure lower statistical errors in the estimates of all of the polarimetric variables—Z_{DR}, ρ_{hv}, Φ_{DP}, and K_{DP}—for the same dwell time (Bringi and Chandrasekar 2001). One of the basic requirements for the operational demonstration was the compatibility of the KOUN antenna-scanning strategy with the standard volume coverage patterns (VCPs) that are currently employed for Next-Generation Weather Radar (NEXRAD) operations. Most data during the spring of 2003 were collected following the VCP-11 scanning strategy, which includes 14 elevation sweeps from 0.5° to 19.5° and a volume update time of about 6 min.

As part of JPOLE, considerable KOUN data were acquired in tornadic storms. In particular, May 2003 was an active storm month with several damaging tornadoes occurring near KOUN. Most notable were the afternoons and evenings of 8 and 9 May when violent tornadoes struck the Oklahoma City metropolitan area.

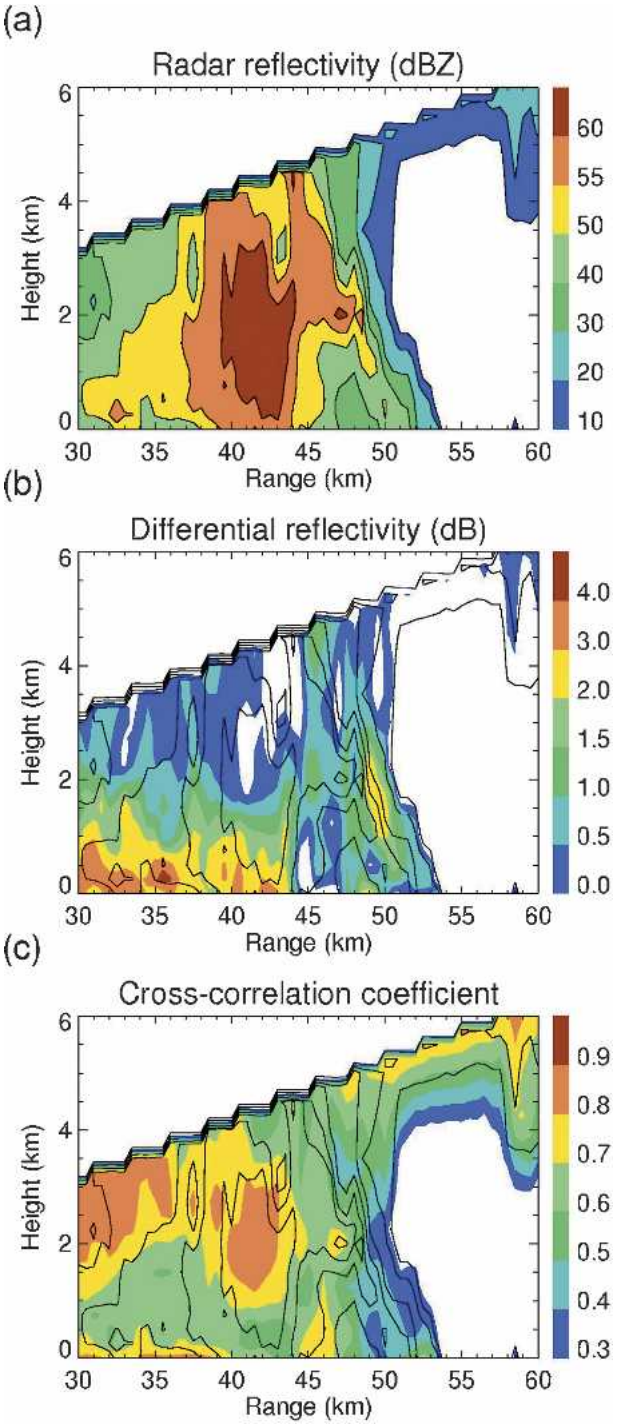

FIG. 3. Vertical cross section of Z, Z_{DR}, and ρ_{hv} corresponding to azimuthal direction 203° (shown in Fig. 2) at 2305 UTC 3 May 1999. A debris signature is centered at 49.5 km from the radar.

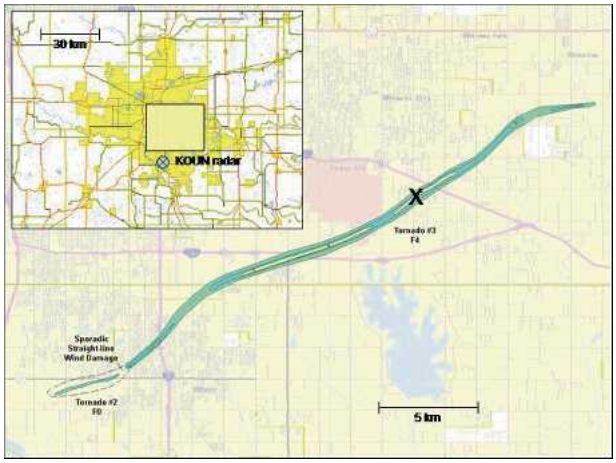

FIG. 4. A damage path map for the 8 May 2003 Oklahoma City area tornado. The cross indicates the location of the tornado at 2229 UTC (see Fig. 5). The areas with different damage intensity in the Fujita scale are shown with colors and contours. The region in the map is shown as a rectangle in the larger-scale map of the Oklahoma City metropolitan area in the inset.

On 8 May 2003, a destructive F4 tornado hit Moore, southeast Oklahoma City, Midwest City, and Choctaw, Oklahoma, creating a 27-km damage path (see Fig. 4). The tornado was spotted from 2210 to 2238 UTC [1610–1638 central standard time (CST)]. The KOUN radar recorded three full volume scans of data during this period, but they were not continuous because of a power outage. The beginning of tornado at 2210 UTC was well captured by the radar. However, because the first tornado touchdown occurred at a distance of only about 10 km from the radar, the data at the lowest sweeps were heavily contaminated by ground clutter.

A good volume scan of data began at 2229 UTC when the tornado was about 20 km from the radar. The tornado location on the damage track at that time is indicated by the cross in Fig. 4. A composite plot of Z, V, Z_{DR}, and ρ_{hv} at 1.5° elevation is shown in Fig. 5. A tornadic signature at the tip of the hook is marked by Z exceeding 50 dBZ, an obvious presence of a vortex in the Doppler velocity field, Z_{DR} close to zero, and anomalously low ρ_{hv} (less than 0.5). These components of the tornado signature are very similar to what was observed by the Cimarron radar on 3 May 1999. Outside the hook, the highest values of Z_{DR} are associated with low to moderate values of Z in the inflow region, which is an indication of pronounced drop sorting. This is discussed in more detail in section 6.

The vertical extension of the debris signature in the hook is about 500 m, as the composite RHI at azimuth = 25° demonstrates (see Fig. 6, 19–20 km from the radar). Among other notable features in the vertical cross section are the Z_{DR} column at the periphery of a hail core and extensive region of low ρ_{hv} (less than 0.90–0.95) stretching up from the tornado on the ground to the height of 7 km in the updraft portion of the storm. We do not exclude that this unusually low ρ_{hv} might be attributed to the mixture of meteorological particles and light debris that are lofted to the storm's midlevel height by a strong updraft. A vertical column of specific differential phase K_{DP} (Fig. 6c) at distances of 29–31 km from the radar is associated with a major precipitation shaft that is loaded primarily with raindrops and possibly some hail, as can be concluded from the vertical distribution of Z and Z_{DR} (Loney et al. 2002).

A tornadic vortex is a very localized feature. Because of spatial smoothing of radar data as part of data processing and conversion of the data from a polar to Cartesian grid, the corresponding values of radar variables may, therefore, not be correctly represented in the PPI and RHI composite images presented in Figs. 5 and 6. Radial profiles of raw (unprocessed) data, although more affected by measurement noise, better represent extreme values of radar variables that are associated with tornadic debris. An example of such profiles of Z, Z_{DR}, and ρ_{hv} is presented in Fig. 7. The tornadic signature at the distance of 20 km from the radar is characterized by a local reflectivity maximum of 53 dBZ, combined with an unprecedented drop of the cross-correlation coefficient to a level of 0.2! Because of extremely low ρ_{hv}, the corresponding differential reflectivity is quite noisy, but it is definitely lower than in surrounding areas. Additional spatial averaging of Z_{DR} reveals this drop quite clearly (Fig. 5).

4. Tornadic case on 9 May 2003

The next day another strong tornado struck northeast Oklahoma City, Witcher, and rural parts of Jones and Luther, Oklahoma, over a 29-km damage path. The path of the F3 tornado is shown in Fig. 8. According to ground information, the tornado started at 2129 CST and ended at about 2206 CST (0329–0406 UTC 10 May 2003). During this time interval, the tornado was at distances of 35–55 km from the radar. The KOUN radar provided uninterrupted flow of polarimetric data throughout the entire lifetime of the tornado. A tornadic signature was identified during successive volume scans, which were updated every 6 min from 0334 to 0358 UTC.

The tornado was relatively far from the radar, and thus the data at the lowest elevation tilt of 0.5° were not contaminated by ground clutter. The fields of Z, V, Z_{DR}, and ρ_{hv} at the lowest radar scan at 0346 UTC are displayed in Fig. 9. At that moment, a strong classical hook echo had developed with all of the indications of tornado occurrence at the tip of the hook (X = 6.5 km, Y = 38.5 km)—increased Z, a Doppler vortex, anomalously low ρ_{hv}, and negative Z_{DR}.

A remarkable tornadic signature at distances of 39–40 km from the radar is evident in the vertical cross section through the hook echo (Fig. 10). The columns

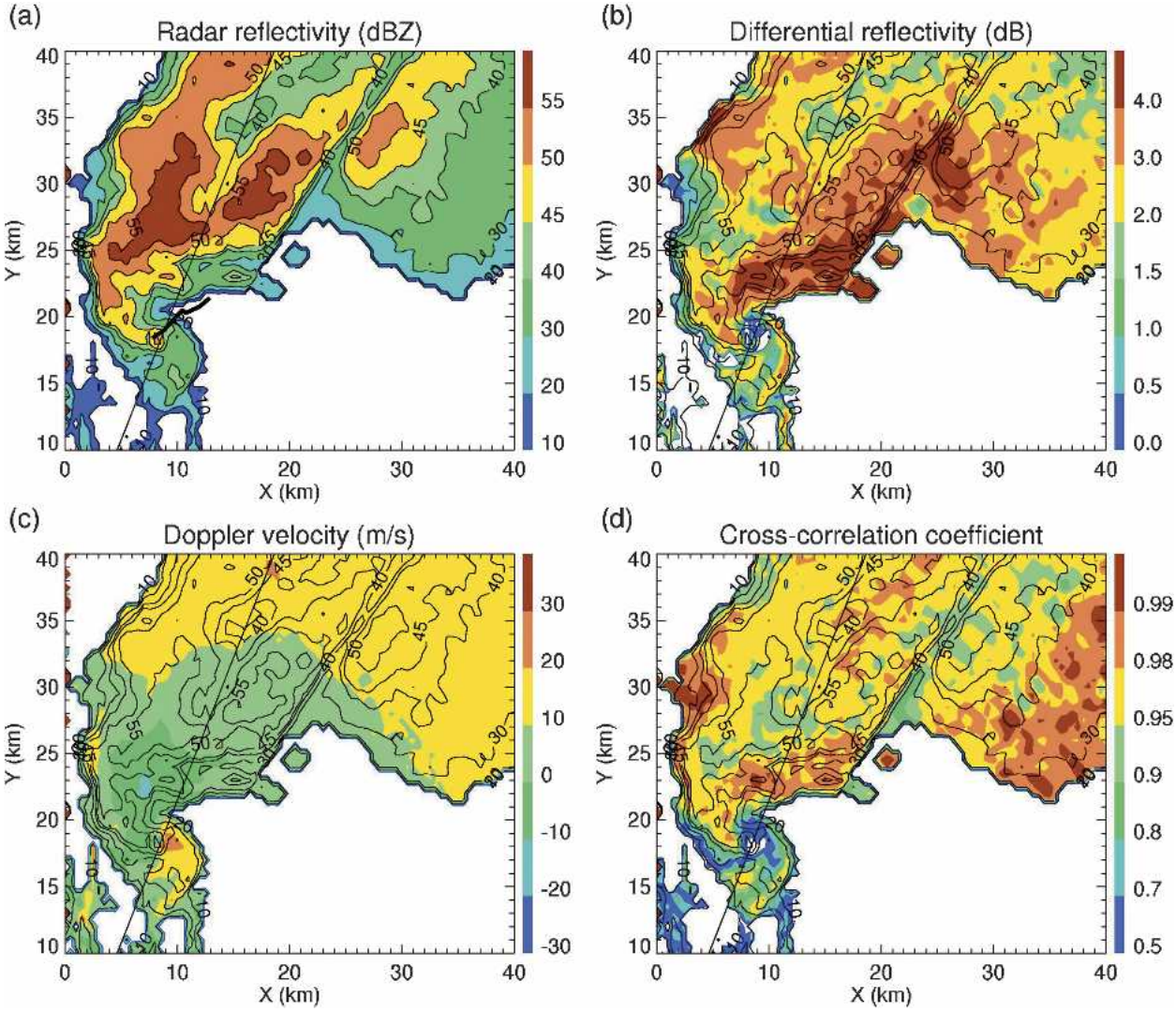

FIG. 5. Fields of Z, Z_{DR}, V, and ρ_{hv} at the PPI scan (1.5°) at 2229 UTC 8 May 2003. Thin solid lines indicate azimuthal direction 25°, and the thick solid line in the Z panel depicts a part of tornado track from the ground observations.

of negative Z_{DR}, negative K_{DP}, and low ρ_{hv} extend vertically from the ground up to a height of 2 km (4 km for ρ_{hv}). The corresponding Z is between 50 and 55 dBZ. There is no doubt that the radar echo in this region is dominated by nonmeteorological scatterers, that is, debris. Negative values of Z_{DR} and K_{DP} might be attributed either to a certain degree of vertical common orientation of the scatterers (if they are relatively small) or to their large size (provided that their orientation is not totally chaotic). In the Mie regime of scattering when the size of scatterers is much larger than the radar wavelength, both Z_{DR} and K_{DP} might have a negative sign even if the horizontal dimension of the scatterers is larger than vertical.

As can be seen from Fig. 10, two distinct columns of enhanced Z that are closely connected aloft and are separated by a "vault" at altitudes below 7.5 km have strikingly different polarimetric attributes. The left column is associated with the rear-flank downdraft (RFD) and exhibits an impressive tilted column of high positive K_{DP}, low values of ρ_{hv} (in comparison with its right counterpart), and highly variable low to moderate Z_{DR}. The right column represents the main precipitation core, consisting of rain below 2–2.5 km and hail above, as can be inferred from Z_{DR}, K_{DP}, and ρ_{hv}. A spectacular Z_{DR} column with maximal Z_{DR} values approaching 6.5 dB is observed in the weak echo region that is associated with the storm updraft.

Analysis of raw data along the radial through the tip of the hook at elevation = 0.5° shows that Z varies between 50 and 57 dBZ, ρ_{hv} drops to approximately 0.60–0.65, and Z_{DR} ranges from −2 to 0 dB in the tornado location at 39–40 km from the radar (Fig. 11). Of note is a tremendous change of Z_{DR} from −2 dB in the

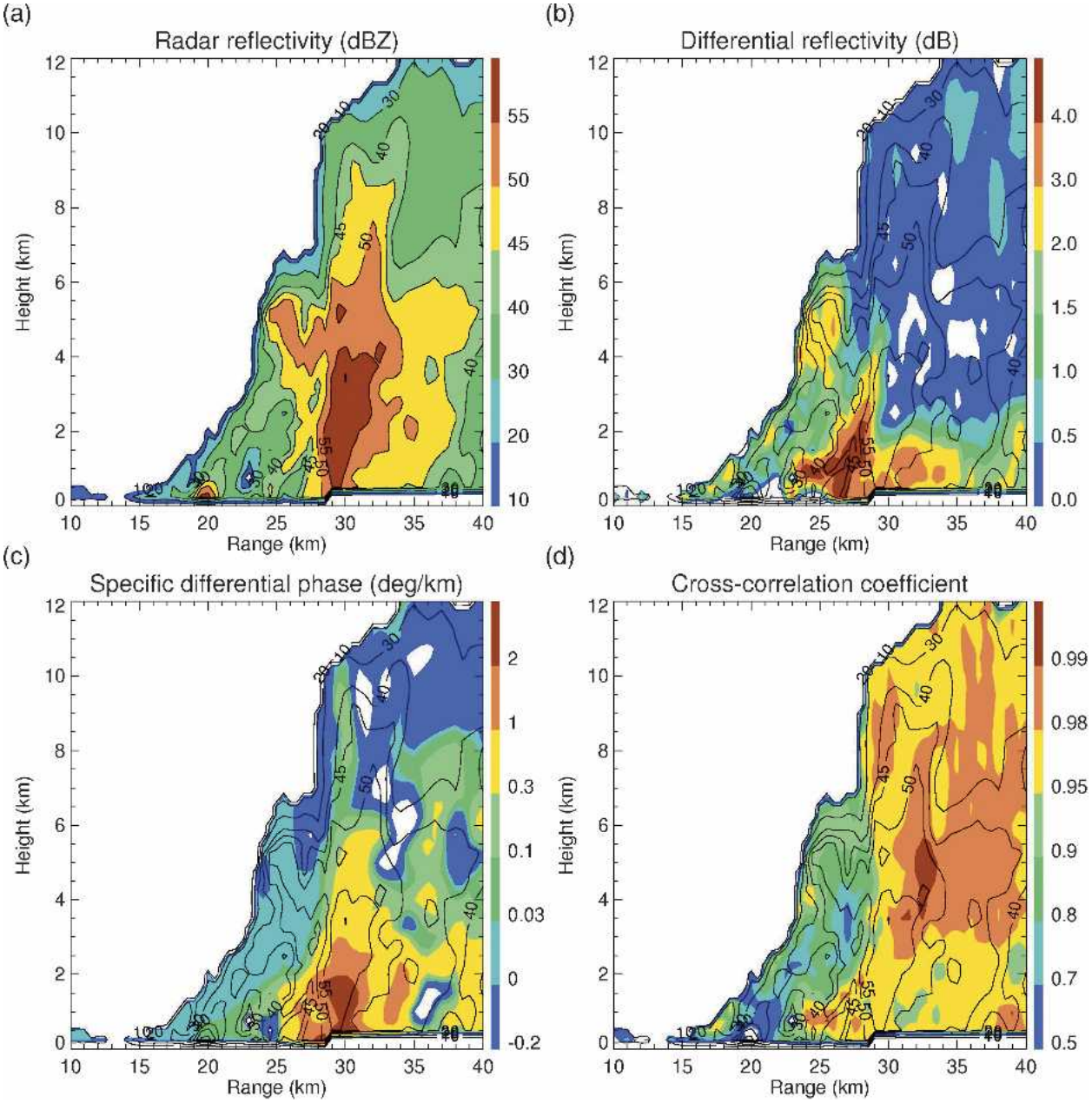

FIG. 6. Vertical cross section of Z, Z_{DR}, K_{DP}, and ρ_{hv}, corresponding to azimuthal direction 25° (shown in Fig. 5) at 2229 UTC 8 May 2003. The debris signature is centered at about 20 km from the radar.

hook echo to 6.4 dB at the edge of the main updraft area and precipitation core (44–45 km).

5. Temporal evolution of the tornadic signatures

For scientific and practical reasons it is definitely desirable to relate tornado signatures to the life cycle of the phenomena. This, however, is beyond the scope of our preliminary investigation. Instead, we document herein the temporal evolution of the signatures for the three tornado cases. Thus, we have examined several consecutive scans of radar data at the lowest available elevations where ground clutter contamination was absent. For each scan, we analyzed the 0.5 km × 0.5 km pixels of Z, Z_{DR}, and ρ_{hv} data in a 20 km × 20 km area that is centered on the hook echo. A pixel where 45 dB$Z < Z <$ 55 dBZ and $\rho_{hv} < 0.8$ is classified as a "ρ_{hv} debris signature." A "Z_{DR} debris signature" is defined with 45 dB$Z < Z <$ 55 dBZ and $Z_{DR} < 0.5$ dB. Because all ρ_{hv} data from the Cimarron radar are negatively

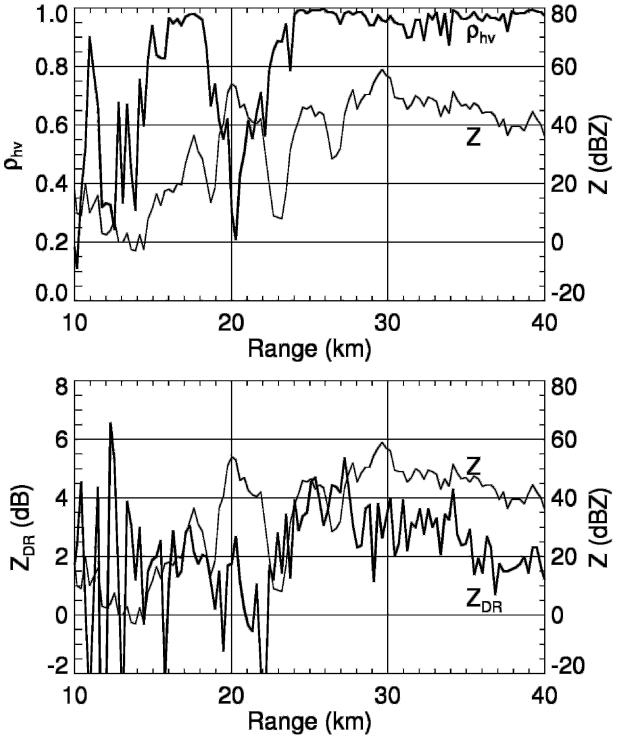

FIG. 7. Radial profiles of raw (unprocessed) Z, Z_{DR}, and ρ_{hv} along the beam through tornado at 2229 UTC 8 May 2003: elevation = 1.5°, azimuth =25°.

biased because of a quantization problem in the radar processor, the ρ_{hv} threshold is lowered to 0.6 for the 3 May 1999 case. Such a threshold, although quite subjective, allows for the elimination of the majority of pixels containing rain, hail, and less reliable data in the weak reflectivity regions at the periphery of the storm

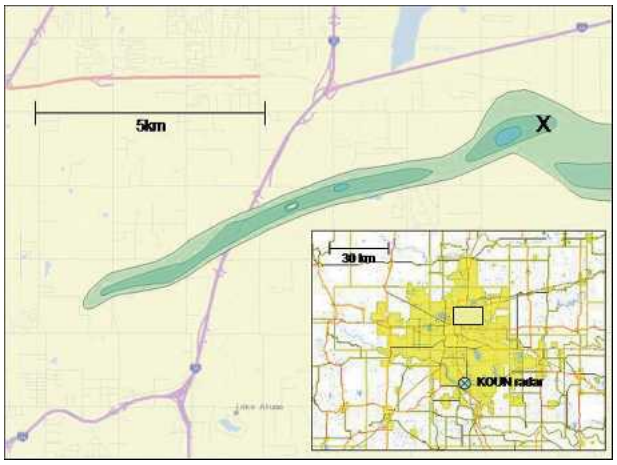

FIG. 8. A damage path map for the 9 May 2003 Oklahoma City area tornado. The cross indicates the location of the tornado at 0346 UTC (10 May, see Fig. 9). The areas with different damage intensity in the Fujita scale are shown with colors and contours.

where both ρ_{hv} and Z_{DR} can be biased by noise. After this designation was made, we counted the number of pixels identified as ρ_{hv} and the Z_{DR} debris signatures and estimate minimal and mean values of ρ_{hv} and Z_{DR} for such pixels [N_{rhv}, N_{zdr}, $\rho_{hv}^{(min)}$, $\langle\rho_{hv}\rangle$, $Z_{DR}^{(min)}$, and $\langle Z_{DR}\rangle$, respectively].

For the three tornadic storms, temporal dependencies of all six parameters characterizing the intensity of the polarimetric debris signature are displayed in Fig. 12. Time intervals during which a tornado was spotted on the ground are shown by gray thick lines at the top of each panel. Radar data were updated every 6 min. As mentioned before, three volume scans are missing between 2210 and 2228 UTC because of a power outage on 8 May 2003, and because the Cimarron radar lost power after 2322 UTC 3 May 1999. Despite these gaps in the data collection, the general evolution of radar signatures is consistent with the results of ground survey. The parameters $\rho_{hv}^{(min)}$, $\langle\rho_{hv}\rangle$, $Z_{DR}^{(min)}$, and $\langle Z_{DR}\rangle$ reach their minima close to the middle of the time intervals when tornadoes were observed, which was also the time of peak tornado intensity. In all three cases the radar did not detect debris before first tornado touchdown occurred. However, on both 8 and 10 May 2003 the radar debris signatures were detected 6–10 min after tornado ended, which is most likely because lofted debris was still in the air.

6. Discussion

Analysis of the three tornadic cases that is presented in this study shows that the polarimetric debris signature is a repeatable feature. The signature exists throughout a tornado's lifetime, provided that the tornado has an intensity of at least F3 according to the Fujita scale. A cursory analysis of other tornadic storms indicates that the majority of the weak tornadoes did not produce definable signatures. One possible reason for this is that wind speeds in weak tornadoes are not sufficient to significantly damage structures and loft debris. Another feasible explanation is that some of the weaker tornadoes may be too short lived. Therefore, a debris signature might have been missed because of coarse temporal sampling.

On the other hand, our study of all of the significant nontornadic supercell storms that were observed during JPOLE does not reveal such a signature. Although Z_{DR} and ρ_{hv} can drop considerably in the middle of hail cores, it is almost impossible to confuse hail and tornado designations because of their location in the storm and the depth of the ρ_{hv} dip. In hail, ρ_{hv} usually does not drop below 0.85 even if hail is large. The only exception in our dataset is an extreme hail event that occurred on 14 May 2003 for which the measured ρ_{hv} in the center of the hail core dropped to as low as 0.75. That was an exceptional hailstorm that produced hail of a 13-cm size!

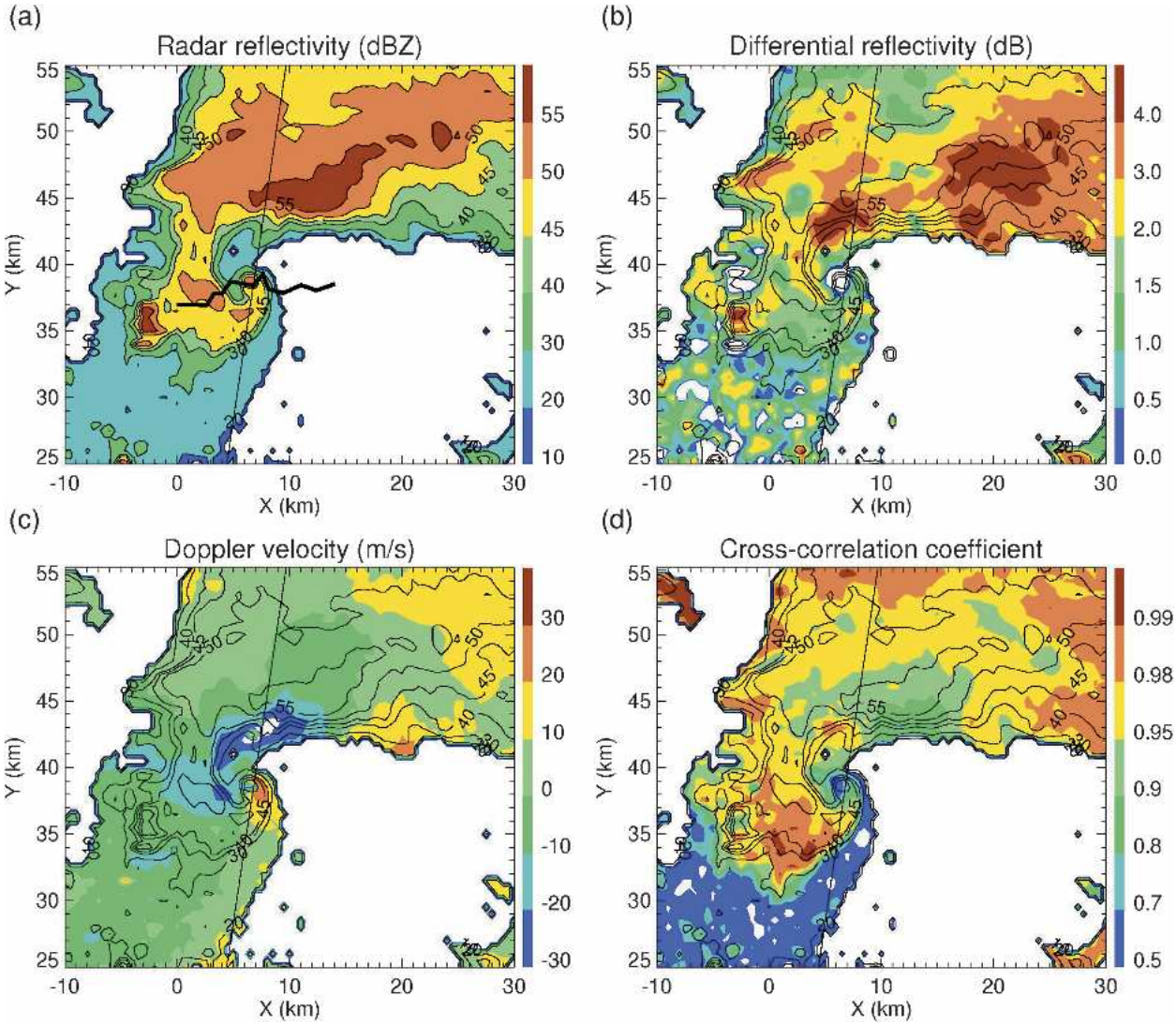

FIG. 9. Fields of Z, Z_{DR}, V, and ρ_{hv} at the PPI scan (0.5°) at 0346 UTC 10 May 2003. Thin solid lines indicate azimuthal direction 10°, and the thick solid line in the Z panel depicts a part of tornado track from the ground observations.

Summarizing our observations of these three events, we can tentatively formulate the following five criteria for polarimetric tornado detection: 1) the presence of a hook echo, 2) $\rho_{hv} < 0.8$, 3) a pronounced vortex signature in the Doppler velocity field, 4) $Z_{DR} < 0.5$ dB, and 5) $Z > 45$ dBZ. If conditions 2–5 are satisfied in the hook area, then it is very likely that a tornado is lofting considerable debris. Among criteria 2–5, criterion 2 probably has the best discriminating power. The cross-correlation coefficient is the most attractive variable because, unlike Z_{DR}, it is not affected by radar miscalibration, attenuation in precipitation, and partial radar beam blockage, provided that the signal-to-noise ratio is sufficiently high. The LDR, considered as a proxy for ρ_{hv}, is vulnerable to all of these conditions.

One reservation regarding the use of ρ_{hv} is that the magnitude of the cross-correlation coefficient is affected by the variability of the differential phase within the radar resolution volume. If a gradient of Φ_{DP} across the radar beam is high and the radar sampling volume is too large, then ρ_{hv} noticeably decreases. This factor explains an observed general decrease of ρ_{hv} with distance, especially if a propagation path contains a large amount of precipitation. Hence, the ρ_{hv} threshold in criterion 2 might depend on range and Φ_{DP}.

The debris signatures can be very useful to confirm tornado warnings and tornado damage, and to pinpoint the current tornado location. Although tornado detection is important, its prediction and early warning are even more important. A cursory look into evolution of the 3D pattern of polarimetric variables in a tornadic supercell reveals quite unusual and intriguing polarimetric signatures aloft, and, in the near proximity of the storm, that might be related to tornado development.

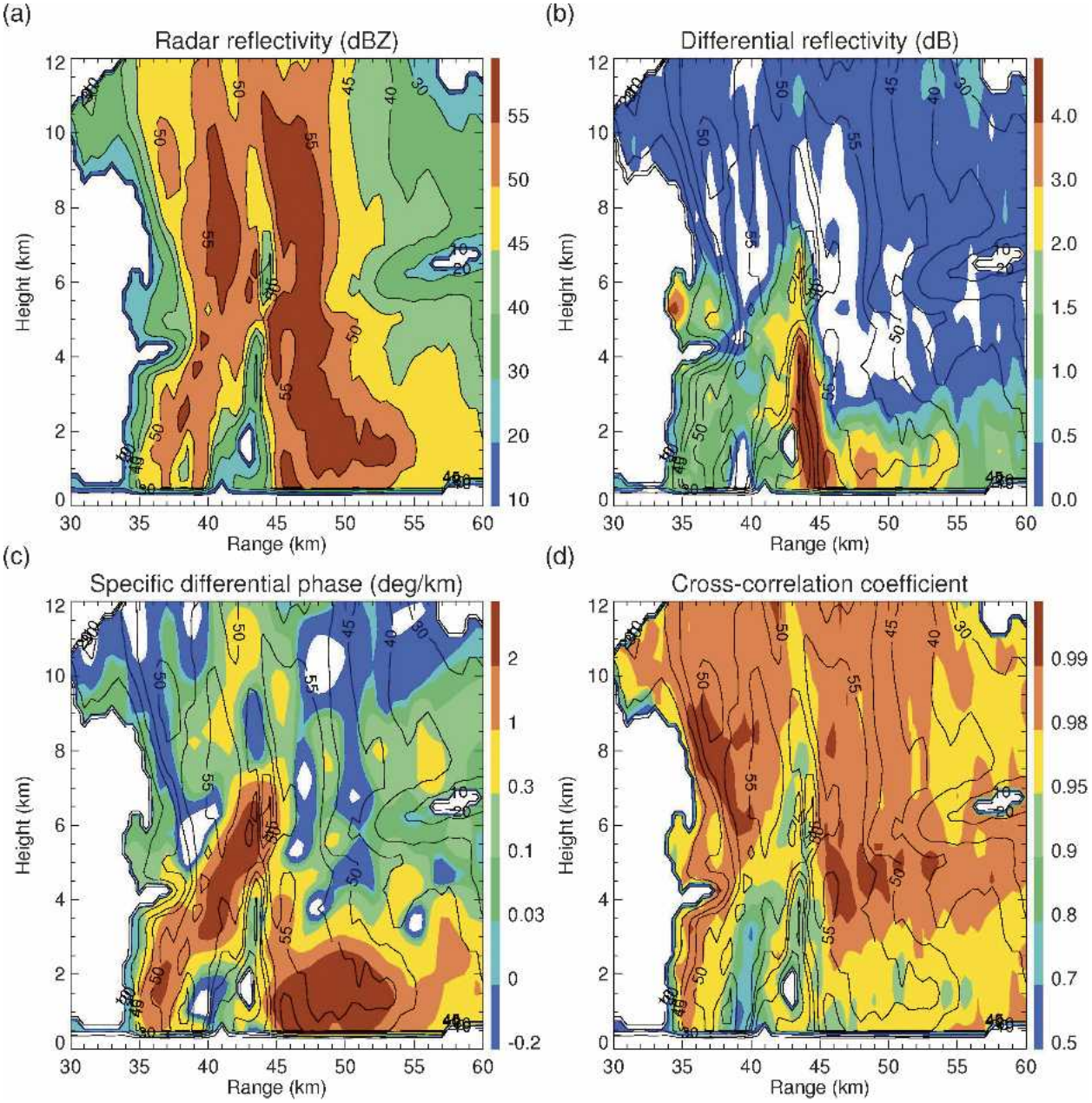

FIG. 10. Vertical cross section of Z, Z_{DR}, K_{DP}, and ρ_{hv} corresponding to azimuthal direction 10° (shown in Fig. 9) at 0346 UTC 10 May 2003. A debris signature is centered at about 39.5 km from the radar.

Similar to the debris signature, these polarimetric patterns are also repetitive and require microphysical interpretation.

Very high values of Z_{DR} exceeding 4 dB are regularly observed at the periphery of high-reflectivity areas ahead of the FFD and in the inflow region (see Figs. 2, 5, and 9). As was already mentioned, the Z_{DR} signature in the FFD area is usually shallow, whereas the one associated with inflow and updraft has a large vertical extent (Figs. 3, 6, and 10). This can be seen very well in a PPI at the higher elevation of 3.5° for the case of 9 May 2003 (Fig. 13). At midlevel heights (2.5–3 km) outside of the inflow and updraft regions, low values of Z_{DR} signify hail, graupel, and snow. A comma-shaped high-Z_{DR} signature in the updraft region is likely attributed to large supercooled drops or melting hailstones.

Anomalously high Z_{DR} can be explained by intense drop sorting in the presence of strong wind shear and mesoscale rotation. Indeed, cloud and precipitation particles (liquid drops, graupel, or hail) that originate in high-reflectivity regions aloft fall to the ground with

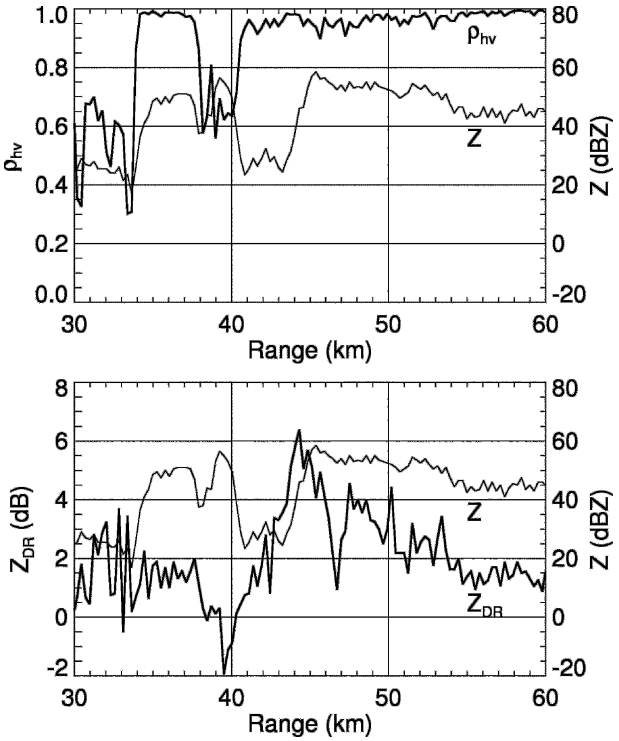

FIG. 11. Radial profiles of raw (unprocessed) Z, Z_{DR}, and ρ_{hv} along the beam through tornado at 0346 UTC 10 May 2003: elevation = 0.5°, azimuth =10°.

very different trajectories, depending on their inertia, that is, size (Browning 1965). Smaller hydrometeors follow the airflow quite well, whereas the larger ones can fall "against the flow" in a highly sheared wind environment. For example, smaller hydrometeors that fall out from the overhang region aloft are easily advected or recirculated back to the cloud by a strong updraft (Conway and Zrnic 1993). In contrast, big particles continue to fall down despite the updraft. Similarly, if the hydrometeors travel in the presence of strong air circulation, then the most massive particles have much better chance to be "centrifuged" away from the center of rotation (Snow 1984; Dowell et al. 2004). The comma-shaped Z_{DR} signature in Fig. 13 that apparently "wraps" a mesoscale vortex points to such a possibility.

In both situations, strong size sorting of hydrometeors takes place and, as a result, the areas adjacent to strong reflectivity cores contain a small number of very large particles (big raindrops or melting hailstones) and lack any small particles. A combination of high oblateness and low concentration produces low Z and high Z_{DR}. A degree of size sorting is directly related to kinematic properties of the storm. Thus, polarimetric signatures might be very useful in the interpretation of dynamical processes in supercell storms.

Intense size sorting affects the cross-correlation coefficient, as well. Drop size distributions that are skewed toward larger sizes are usually characterized by lower ρ_{hv}. In addition, the presence of nonmeteorological scatterers (including debris) in a mixture with hydrometeors further depresses ρ_{hv}. Very low measured values of ρ_{hv} in the updraft regions for all three examined tornadic storms indicate that large portions of updraft contain light debris, such as leaves, grass, and dust. The magnitude of ρ_{hv} and the vertical extent of the low ρ_{hv} signatures in updrafts provide indirect measure of their strength, which is quite difficult to estimate from conventional Doppler measurements. One has to be cautious, however, regarding the interpretation of ρ_{hv} that can be negatively biased because of enhanced gradients of differential phase within the radar resolution volume.

Once light debris is lofted to higher levels in a tornadic storm, it takes some time (tens of minutes) for debris to sediment to the ground (Magsig and Snow 1998). Suspended light debris is the most reasonable explanation of the supercell storm "wake" signature that is usually observed in the wake of the strong low-level wind field behind the storm (see Fig. 9). It is characterized by low Z (less than 30 dBZ), low ρ_{hv} (less than 0.7), and mean Z_{DR} varying between 1 and 2 dB. Low values of ρ_{hv} point to nonmeteorological scatterers as a source of echo. Ground clutter is excluded because the Doppler velocity is far from zero, and Z_{DR} is mainly positive, whereas it is usually slightly negative for ground targets. Biological scatterers, like insects and birds, have a much higher Z_{DR} and quite a different differential phase upon scattering δ. The observed δ in the "wake" echo is about 50°–60°, which is different from the one that is typical for insects (10°–40°) and birds (70°–100°) (Zrnic and Ryzhkov 1998; Schuur et al. 2003). Hence, lofted light debris with a certain degree of common alignment (probably leaves and grass) remains the only feasible explanation for such an echo.

7. Conclusions

All previous observational studies of tornadoes that were made with Doppler radars emphasized the kinematic properties of storms (see a review by Markowski 2002). For the first time we have obtained strong evidence that a dual-polarizaton radar can effectively complement Doppler information and provide additional tornado detection capabilities. Three major tornadic storms that hit the Oklahoma City metropolitan area in recent years all exhibit well-defined polarimetric debris signatures that are characterized by an unprecedented drop in the cross-correlation coefficient ρ_{hv} and differential reflectivity Z_{DR} in the hook echo. Such signatures are less pronounced for weaker tornadoes, but reliably identify tornadoes rated as F3 in the Fujita scale.

The debris signature that is associated with tornadic touchdown is quite small with a horizontal size of about 1 km and vertical extent of 1–3 km. Doppler measurements require good spatial resolution in order to re-

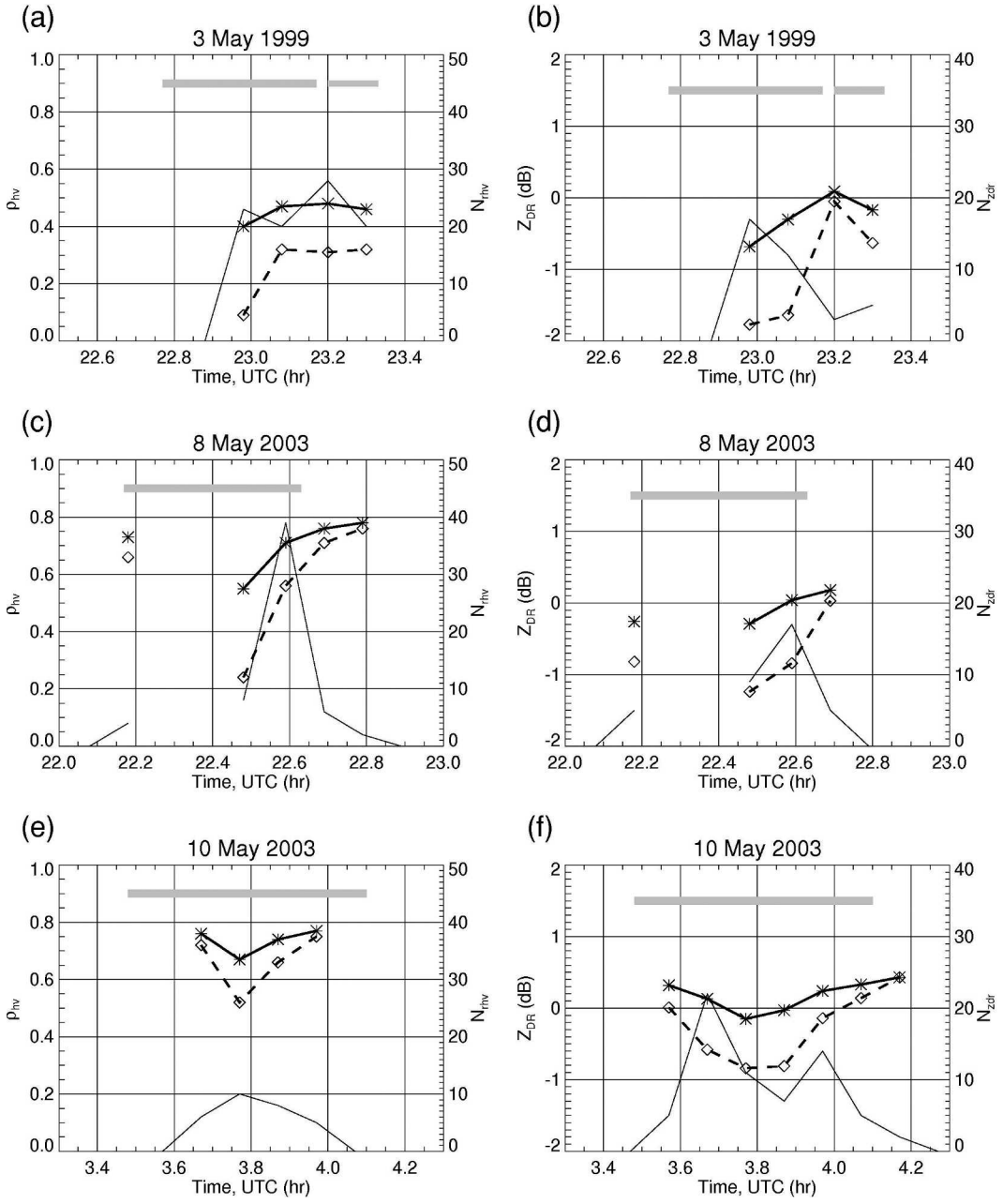

FIG. 12. Temporal dependencies of ρ_{hv} and Z_{DR} associated with debris signatures during three tornado events. (a), (c), (e) Thick solid lines and stars depict average ρ_{hv} in the 0.5 km $\times$ 0.5 km pixels where 45 dB$Z < Z <$ 55 dBZ and $\rho_{hv} < 0.8$; thick dashed lines and diamonds denote minimal value of ρ_{hv}; thin lines indicate the number of such pixels. (b), (d), (f) Thick solid lines and stars depict average Z_{DR} in the 0.5 km $\times$ 0.5 km pixels where 45 dB$Z < Z <$ 55 dBZ and $Z_{DR} < 0.5$ dB; thick dashed lines and diamonds denote minimal value of Z_{DR}; thin lines indicate the number of such pixels. Time intervals during which the tornado was spotted on the ground are shown by gray thick lines at the top of each panel.

solve a small tornado vortex, whereas identification of polarimetric signatures can be accomplished with a coarser resolution. Moreover, these signatures are "isotropic" in their nature. That is, as opposed to Doppler velocities, they do not depend on a viewing angle.

Although a very small tornado signature might not be well resolved at long distances from the radar, larger-scale polarimetric signatures, associated with light debris (leaves, grass, etc.) that is lofted in the cloud by a strong updraft, as well as intense size sorting of hydrometeors might be helpful to diagnose the current state of the supercell storm and its potential ability to

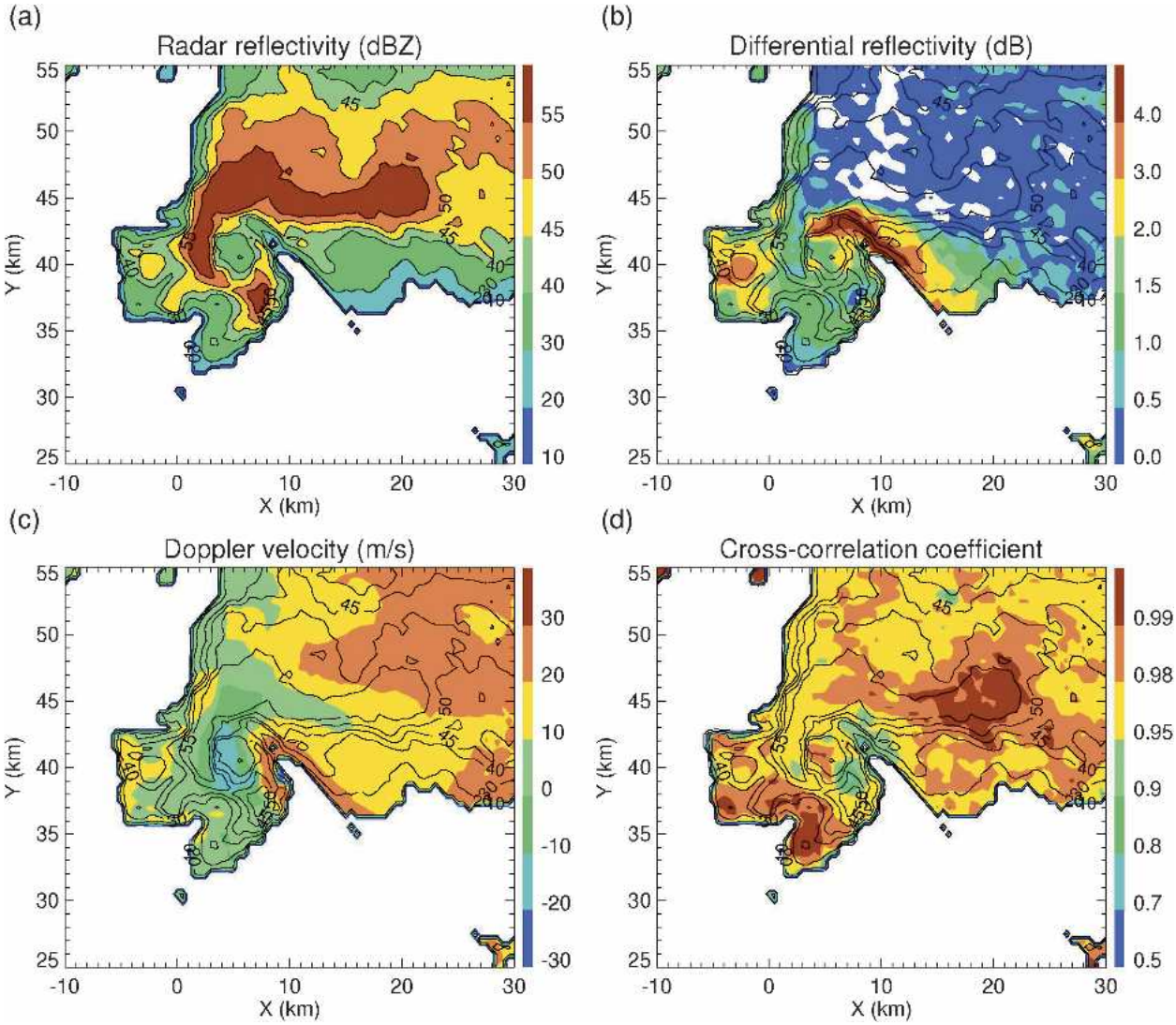

FIG. 13. Fields of Z, Z_{DR}, V, and ρ_{hv} at the PPI scan (3.5°) at 0346 UTC 10 May 2003.

produce a tornado. Light debris in the inflow region of the storm and in its wake is associated with low values of ρ_{hv} and a sizeable differential phase upon scattering, whereas size sorting is manifested by very high values of Z_{DR}. Both larger-scale polarimetric signatures provide indirect estimates of the strength of vertical flows and circulation within the storm.

In cases in which traditional Doppler tornado-warning signatures are absent or overlooked by forecasters, the polarization tornado signature might be very valuable in preventing what otherwise might have been a missed warning. This signature might also be very helpful in issuing accurate severe weather–warning updates to pinpoint the current tornado location and confirm the occurrence of damage (based on debris).

A cursory look into evolution of the 3D pattern of polarimetric variables prior to tornadic touchdown reveals quite unusual and intriguing polarimetric signatures aloft that might be related to the development of a subsequent tornado. Understanding and interpretation of these signatures could provide insight into microphysical aspects of tornadogenesis.

Acknowledgments. This work would not have been possible without the dedicated support from the NSSL and CIMMS/University of Oklahoma staff that maintains the Cimarron and KOUN WSR-88D.

The authors acknowledge funding support for this work from the U.S. National Weather Service, the Federal Aviation Administration, and the U.S. Air Force Weather Agency through the NEXRAD Products Improvement Program.

REFERENCES

Bringi, V. N., and V. Chandrasekar, 2001*: Polarimetric Doppler Weather Radar: Principles and Applications.* Cambridge University Press, 636 pp.

Browning, K. A., 1965: Some inferences about the updraft within a severe local storm. *J. Atmos. Sci.,* **22,** 669–678.

Burgess, D. B., M. A. Magsig, J. Wurman, D. C. Dowell, and Y. Richardson, 2002: Radar observations of the 3 May 1999 Oklahoma City tornado. *Wea. Forecasting,* **17,** 456–471.

Conway, J. W., and D. S. Zrnic, 1993: A study of embryo production and hail growth using dual-Doppler and multiparameter radar. *Mon. Wea. Rev.,* **121,** 2511–2528.

Dowell, D. C., C. R. Alexander, J. M. Wurman, and L. J. Wicker, 2005: Centrifuging of hydrometeors and debris in tornadoes: Radar-reflectivity patterns and wind-measurement errors. *Mon. Wea. Rev.,* **133,** 1501–1524.

Gorgucci, E., G. Scarchilli, and V. Chandrasekar, 1999: A procedure to calibrate multiparameter weather radar using properties of the rain medium. *IEEE Trans. Geosci. Remote Sens.,* **37,** 269–276.

Hubbert, J., V. N. Bringi, and L. D. Carey, 1998: CSU-CHILL polarimetric measurements from a severe hail storm in eastern Colorado. *J. Appl. Meteor.,* **37,** 749–775.

Loney, M. L., D. S. Zrnic, J. M. Straka, and A. V. Ryzhkov, 2002: Enhanced polarimetric radar signatures above the melting level in supercell storm. *J. Appl. Meteor.,* **41,** 1179–1194.

Magsig, M. A., and J. T. Snow, 1998: Long-distance debris transport by tornadic thunderstorms. Part I: The 7 May 1995 supercell thunderstorm. *Mon. Wea. Rev.,* **126,** 1430–1449.

Markowski, P. M., 2002: Hook echoes and rear-flank downdrafts: A review. *Mon. Wea. Rev.,* **130,** 852–876.

Ryzhkov, A. V., and D. S. Zrnic, 1995: Precipitation and attenuation measurements at a 10-cm wavelength. *J. Appl. Meteor.,* **34,** 2121–2134.

——, D. W. Burgess, D. S. Zrnic, T. Smith, and S. E. Giangrande, 2002a: Polarimetric analysis of a 3 May 1999 tornado. Preprints, *21st Conf. on Severe Local Storms*, San Antonio, TX, Amer. Meteor. Soc., 515–518.

——, S. E. Giangrande, D. S. Zrnic, 2002b: Using multiparameter data to calibrate polarimetric weather radars in the presence of a partial beam blockage. *Proc. IGARSS 2002*, Toronto, ON, Canada, 2820–2822.

Schuur, T. J., A. V. Ryzhkov, P. L. Heinselman, D. S. Zrnic, D. W. Burgess, and K. A. Scharfenberg, 2003: Observations and classification of echoes with the polarimetric WSR-88D radar. NSSL Rep., 46 pp. [Available online at http://www.nssl.noaa.gov/88d-upgrades/WSR-88D_reports.html.]

Snow, J. T., 1984: On the formation of particle sheaths in columnar vortices. *J. Atmos. Sci.,* **41,** 2477–2491.

Vivekanandan, J., D. S. Zrnic, S. M. Ellis, D. Oye, A. V. Ryzhkov, and J. Straka, 1999: Cloud microphysics retrieval using S-band dual-polarization radar measurements. *Bull. Amer. Meteor. Soc.,* **80,** 381–388.

Zahrai, A., and D. S. Zrnic, 1993: The 10-cm wavelength polarimetric weather radar at NOAA's National Severe Storms Laboratory. *J. Atmos. Oceanic Technol.,* **10,** 649–662.

Zrnic, D. S., and A. V. Ryzhkov, 1998: Observations of insects and birds with a polarimetric radar. *IEEE Trans. Geosci. Remote Sens.,* **36,** 661–668.

——, and ——, 1999: Polarimetry for weather surveillance radars. *Bull. Amer. Meteor. Soc.,* **80,** 389–406.